OPEN ACCESS Freely available online

PLOS | COMPUTATIONAL BIOLOGY

A Multi-scale Analysis of Influenza A Virus Fitness Trade-offs due to Temperature-dependent Virus Persistence

Andreas Handel[1]*, Justin Brown[2], David Stallknecht[2], Pejman Rohani[3,4,5]

1 Department of Epidemiology and Biostatistics, College of Public Health, University of Georgia, Athens, Georgia, United States of America, **2** Department of Population Health, College of Veterinary Medicine, The University of Georgia, Athens, Georgia, United States of America, **3** Department of Ecology and Evolutionary Biology, University of Michigan, Ann Arbor, Michigan, United States of America, **4** Center for the Study of Complex Systems, University of Michigan, Ann Arbor, Michigan, United States of America, **5** Fogarty International Center, National Institutes of Health, Bethesda, Maryland, United States of America

Abstract

Successful replication within an infected host and successful transmission between hosts are key to the continued spread of most pathogens. Competing selection pressures exerted at these different scales can lead to evolutionary trade-offs between the determinants of fitness within and between hosts. Here, we examine such a trade-off in the context of influenza A viruses and the differential pressures exerted by temperature-dependent virus persistence. For a panel of avian influenza A virus strains, we find evidence for a trade-off between the persistence at high versus low temperatures. Combining a within-host model of influenza infection dynamics with a between-host transmission model, we study how such a trade-off affects virus fitness on the host population level. We show that conclusions regarding overall fitness are affected by the type of link assumed between the within- and between-host levels and the main route of transmission (direct or environmental). The relative importance of virulence and immune response mediated virus clearance are also found to influence the fitness impacts of virus persistence at low versus high temperatures. Based on our results, we predict that if transmission occurs mainly directly and scales linearly with virus load, and virulence or immune responses are negligible, the evolutionary pressure for influenza viruses to evolve toward good persistence at high within-host temperatures dominates. For all other scenarios, influenza viruses with good environmental persistence at low temperatures seem to be favored.

Citation: Handel A, Brown J, Stallknecht D, Rohani P (2013) A Multi-scale Analysis of Influenza A Virus Fitness Trade-offs due to Temperature-dependent Virus Persistence. PLoS Comput Biol 9(3): e1002989. doi:10.1371/journal.pcbi.1002989

Editor: Christophe Fraser, Imperial College London, United Kingdom

Received August 22, 2012; **Accepted** February 4, 2013; **Published** March 21, 2013

Funding: PR was supported by the James S. McDonnell Foundation, the National Science Foundation (DEB-0917853) and the RAPIDD program of the Science and Technology Directorate, Department of Homeland Security, and the Fogarty International Center, National Institutes of Health. JB was supported by the National Institute of Allergy and Infectious Diseases, National Institutes of Health, Department of Health and Human Services, under Contract No. HHSN266200700007C. The funders had no role in study design, data collection and analysis, decision to publish, or preparation of the manuscript. The opinions expressed herein are those of the author(s) and do not necessarily reflect the views of any of the funding agencies.

Competing Interests: The authors have declared that no competing interests exist.

* E-mail: ahandel@uga.edu

Introduction

Influenza A viruses infect both humans and animals, causing frequent outbreaks [1,2]. In humans, the infection can be life-threatening for individuals with weak immune systems, leading to an estimated annual worldwide mortality burden of $\sim$500,000 [3,4]. Due to its zoonotic nature, and frequent spillover from wild and livestock populations, eradication of the virus is virtually impossible [1,5]. Further, the danger that a novel influenza strain with high virulence and pandemic potential will start to spread in the human population is always present [6–8]. The 2009 H1N1 pandemic demonstrated that the emergence of novel pandemic strains is still largely unpredictable. Improvement of our surveillance, prediction and control capabilities requires that we obtain a better understanding of the whole transmission cycle of the virus and the mechanisms governing the complex processes of infection and spread.

One useful approach for studying the whole infection and transmission process is through the use of multiscale studies, wich have seen increased general development and use in recent years (see e.g. [9,10] for reviews and [11] for a recent application to influenza). A multiscale approach allows one to address the question of how different selection pressures on the within- and between-host levels interact to impact overall fitness. This is important if we want to better understand and predict the infection and transmission dynamics and evolution of the virus.

Here, we use such a multiscale framework and focus on one specific aspect, namely evolutionary pressures shaped by temperature-dependent virus persistence. The importance of temperature on influenza virus fitness is well established. For instance, the attenuated live influenza vaccine is cold-adapted, which leads to reduced fitness in human hosts, making it safe for vaccination purposes [12,13]. Temperature has also been shown to impact within-host dynamics and transmission in laboratory studies [14,15]. Recent theoretical and experimental evidence suggests that persistence in the environment is an important factor of transmission for avian influenza [16–24]. Transmission through an environmental stage (e.g. long-lasting droplets, fomites) seems to also play a role for influenza transmission in humans [25–29]. Since temperatures in the environment and within a host can be markedly different, it is possible that the virus faces a trade-off: It can either optimize its ability to persist within a host, or optimize

Author Summary

It has recently been suggested that for avian influenza viruses, prolonged persistence in the environment plays an important role in the transmission between birds. In such situations, influenza virus strains may face a trade-off: they need to persist well in the environment at low temperatures, but they also need to do well inside an infected bird at higher temperatures. Here, we analyze how potential trade-offs on these two scales interact to determine overall fitness of the virus. We find that the link between infection dynamics within a host and virus shedding and transmission is crucial in determining the relative advantage of good low-temperature versus high-temperature persistence. We also find that the role of virus-induced mortality, the immune response and the route of transmission affect the balance between optimal low-temperature and high-temperature persistence.

its ability to persist outside a host. It is well known that the decay rate of most viruses depends on temperature, with faster virion decay occurring at higher temperature [30–32]. Interestingly, recent data [33] suggest that temperature-dependent decay rates differ between influenza strains. Some strains are very stable at environmental temperatures ($\approx 5-20^{\circ}\mathrm{C}$) but rapidly decay at higher within-host temperatures ($\approx 35-40^{\circ}\mathrm{C}$), while others persist less well at low temperatures but also have a less rapid decay as temperature increases [33]. These data suggest that some virus strains might optimize persistence within a host, while others might optimize persistence outside a host, with a possible trade-off between the two. This in turn can affect both within-host and between-host dynamics. The dynamics on these two levels interact to determine overall fitness. (Note that the data presented in [33] – which we will analyze below – is for different HA-NA serotypes. However, the phenomenon of temperature-dependent decay we discuss is not specific to distinct serotypes. We will therefore use the generic term "strain" throughout this study).

To analyze the impact that such a temperature-dependent trade-off can have on virus fitness, we build a multi-scale model that embeds a within-host infection process within a population transmission framework. A number of theoretical studies have previously considered trade-offs between environmental persistence and within-host performance, see e.g. [34–38]. Those studies considered generic trade-offs and models without direct relation to a specific pathogen or fitting to data. A few notable studies that involved data looked at environmental survival and virulence of human pathogens [39] and environmental survival and growth in phages [40]. Here, we focus on avian influenza A and combine experimental data with models to explicitly consider temperature-dependent virus decay as the mediator of trade-offs. We find that for direct transmission scenarios, viruses with long within-host persistence perform overall best. For environmental transmission scenarios, the balance was shifted toward viruses with good environmental persistence. This was especially true if shedding or infection rates were assumed to be proportional to the logarithm of the virus load. We further show that the addition of an immune response or pathogen virulence reduced the importance of differences in the within-host decay rate between strains, and lead to an increased importance of good environmental persistence.

Models

The within-host model

We consider a simple model for an acute viral infection. These types of models have been used in several recent analyses of influenza A virus within-host infection dynamics (see e.g. [41,42] for reviews). Our model tracks uninfected cells, U, infected cells, X, and infectious virus, V. Cells become infected at rate k, infected cells produce virus at rate p and die at rate δ. Infectious virus decays at rate c_w. The model equations are given by

$$\frac{dU}{dt} = -kUV \quad \text{uninfected cells} \tag{1}$$

$$\frac{dX}{dt} = kUV - \delta X \quad \text{infected cells} \tag{2}$$

$$\frac{dV}{dt} = pX - c_w V \quad \text{virus} \tag{3}$$

The model is illustrated in figure 1, table 1 summarizes the model variables and parameters.

This simple model can describe most data for influenza virus infections rather well [41,42]. After an initial rise in virus load, uninfected target cells become depleted, leading to a subsequent virus decline and resolution of the infection. This so-called target-cell limited model is basically equivalent to a simple epidemic model, which produces a single infectious disease outbreak in a susceptible population. However, it is also known that influenza infections stimulate an immune response, which likely plays some role in viral clearance, though the exact contributions of various components of the immune response to virus clearance are still not fully understood. We consider an alternative model with an immune response in the supplementary materials.

The between-host model

To describe influenza transmission dynamics on the between-host level, we use a framework that takes into account both direct and environmental transmission routes, as has been recently advocated [16,17]. Similar models – not specific to influenza – that explicitly include an environmental stage have been designed and analyzed previously [35,36,38,43–46].

We use coupled partial differential equations to allow for explicit tracking of the age of infection within the infected population. This allows for convenient linking of the within- and between-host scales as described below. The model is shown and explained in figure 2 and legend, table 2 summarizes model quantities. The model equations are given by

$$\frac{dS(t)}{dt} = -S(t)\left(b_2 P(t) + \int_0^\infty b_1(a) I(t,a) da\right) \quad \text{susceptible hosts} \tag{4}$$

$$I(t,0) = S(t)\left(b_2 P(t) + \int_0^\infty b_1(a) I(t,a) da\right) \quad \text{newly infected hosts} \tag{5}$$

$$\frac{\partial I(t,a)}{\partial t} = -\frac{\partial I(t,a)}{\partial a} - g(a) I(t,a) \quad \text{infected hosts} \tag{6}$$

$$\frac{dP}{dt} = \int_0^\infty w(a) I(t,a) da - c_b P \quad \text{virus in the environment} \tag{7}$$

Time t indicates the usual "system time", while a indicates the time since infection of a host. The parameters $b_1(a)$, $w(a)$ and $g(a)$, i.e. the

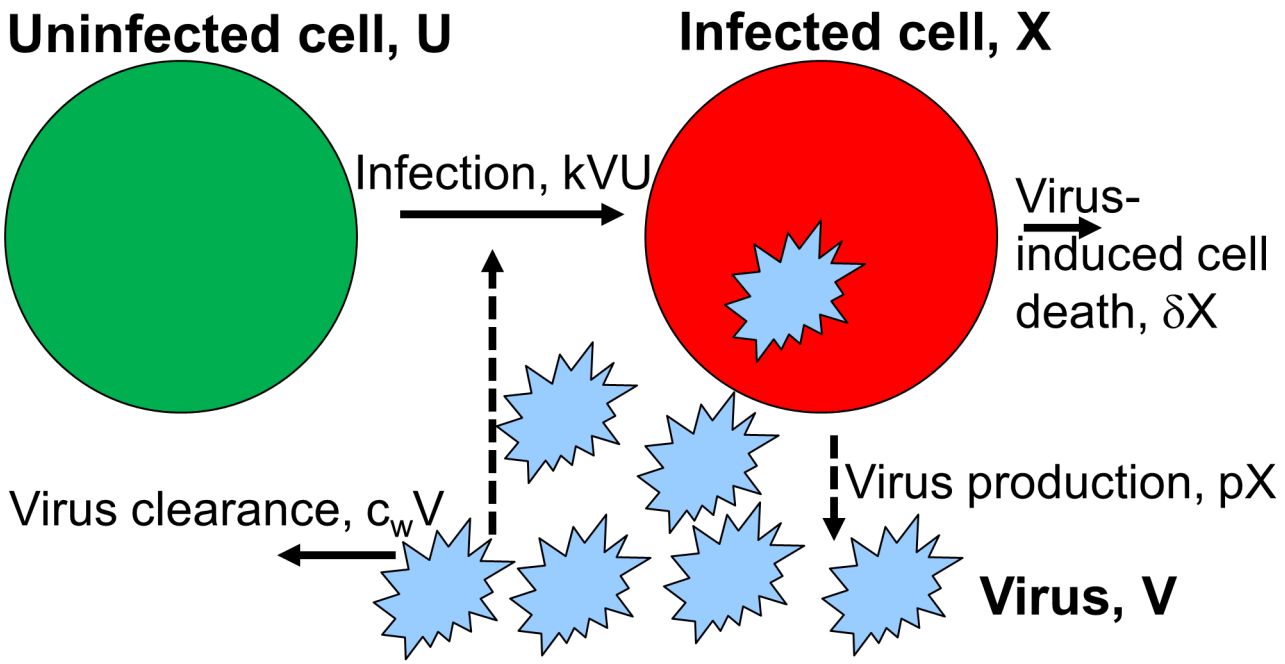

Figure 1. Flow diagram for the within-host model. U, X, and V are the variables describing uninfected cells, infected cells, and infectious virus. Uninfected cells become infected at rate k, infected cells produce virus at rate p and die at rate δ. Virus decays at rate c_w. Solid lines indicate physical flows, dashed lines indicate interactions.
doi:10.1371/journal.pcbi.1002989.g001

rate of transmission between hosts, the rate of shedding and the rate of recovery all depend on the time since infection. We will choose specific forms for those parameters in the next section.

Note that we do not actually simulate the between-host dynamical process. The reason for specifying the between-host model is to compute the basic reproductive number, R_0, which is our measure of between-host fitness (see next section). Analysis of other fitness measures that would require simulating the between-host dynamical process (e.g. probability of extinction over multiple outbreaks) is a suitable subject of future studies but will not be considered here.

Defining fitness and connecting the two scales

Our main quantity of interest is fitness of the virus at the host population level. One way to quantify fitness is through the basic reproductive number, R_0, which is defined as the expected number of new infections caused by one infected host in a fully susceptible population [47–49]. For our model, one can split R_0 into two components, namely direct transmission from host to host (R_d), and indirect transmission through the environmental route (R_e), such that $R_0 = R_d + R_e$ [17,36]. For direct transmission, we have

$$R_d = S(0)\int_0^\infty b_1(a)G(a)da, \tag{8}$$

where $S(0)$ is the susceptible population at time 0, $G(a)$ is fraction of hosts that are still infectious at time a after infection started, and $b_1(a)$ denotes the rate at which an infectious individual at infection age a infects new individuals. If we assume that all infected hosts are infectious for a fixed duration, D, and non-infectious afterwards, we can write

$$R_d = S(0)\int_0^D b_1(a)da. \tag{9}$$

Table 1. Initial conditions and parameter values for the within-host model.

symbol	meaning	values	comment
$U(0)$	target cells	2.5×10^7	based on [71]
$I(0)$	initial number of infected cells	0	assumed
$V(0)$	inoculum dose	1 EID_{50}/mL	assumed
c_w	virus clearance rate	2.78 per day	fixed, see text
b	infection rate	2.2×10^{-6} mL/EID_{50} per day	fitted
p	production rate of virions	1.2 EID_{50}/mL per day	fitted
δ	death rate of infected cell	1.9 per day	fitted

Initial conditions and parameter values for the within-host model. EID_{50} = 50% Egg Infectious Dose.
doi:10.1371/journal.pcbi.1002989.t001

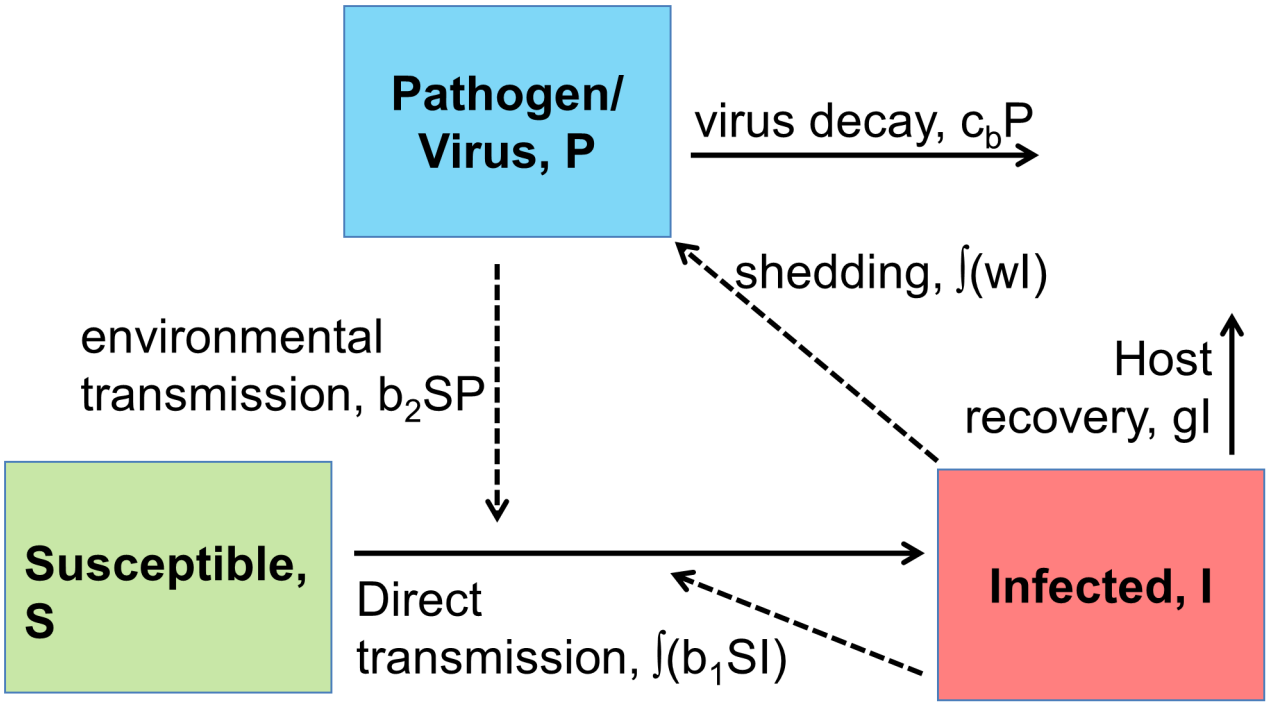

Figure 2. Flow diagram for the between-host model. S, I and P are the variables describing susceptible hosts, infected hosts, and pathogen (i.e. virus) in the environment. Transmission can occur directly between uninfected and infected hosts at rate $b_1(a)$ and through contact of uninfected hosts with virus in the environment at rate b_2. Infected hosts shed virus into the environment at rate $w(a)$, and recover (and are assumed to become immune to re-infection) at rate $g(a)$. Virus in the environment decays at rate c_b. Note that the parameters $b_1(a)$, $w(a)$ and $g(a)$, i.e. the rate of transmission between hosts, the rate of shedding and the rate of recovery all depend on the time since infection. Solid lines indicate physical flows, dashed lines indicate interactions.
doi:10.1371/journal.pcbi.1002989.g002

Mathematically, this corresponds to choosing the proportion of host infectious after time a, $G(a)$, as a Heaviside function, and the recovery rate, $g(a)$, in the between-host model equations as a Dirac delta-function. While the infectious period could end either due to resolution of the infection (recovery) or host death, for the low pathogenic influenza strains we consider here, mortality is negligible [50–52]. Therefore, for the main part of this study, the end of the infectious period should be interpreted biologically as recovery. In the supplementary materials we briefly consider virus-associated mortality (i.e. virulence) and how it might alter the results presented in the main part of the manuscript.

We can define the duration of infectiousness D in terms of the within-host model, as the time from the start until the end of the infection, which we define as the time virus levels drop below a given level, V_D (in our simulations chosen to be one virion). Mathematically, this can be written as

$$D = \min_t (V(t) \leq V_D) \tag{10}$$

The rate at which direct transmission between hosts occurs, $b_1(a)$, also likely depends on the within-host dynamics. One possible assumption is that $b_1(a)$ is directly proportional to virus load:

$$b_1(a) = h_1 V(a), \tag{11}$$

where $V(a)$ is the virus load at time a after infection and h_1 is some constant of proportionality. This assumption corresponds to the "flu like infection regime" in [53], and seems to be a reasonable approximation [54–57]. Defining

$$s_1 = \int_0^D V(a)da \tag{12}$$

as the total infectious virus during the infection (area under the curve), and substituting equations (12) and (11) into (9), we obtain as expression for the directly transmitted virus fitness

$$R_d = S(0)h_1 s_1. \tag{13}$$

While a linear relationship between transmission and virus load, as described by equation (12), is plausible, it is certainly not the only possibility. For instance, we previously showed

Table 2. Parameters for the between-host model.

symbol	meaning
b_2	environmental infection rate
c_b	virus decay rate in the environment
$b_1(a)$	direct transmission rate*
$g(a)$	rate of recovery*
$w(a)$	rate of shedding*

Parameters for the between-host model. Parameters marked with * depend on time a since start of infection. Specific choices for these parameters are described in the text. Note that we do not make use of specific numeric values for any of these parameters, therefore none are given.
doi:10.1371/journal.pcbi.1002989.t002

that a sigmoid function of the form

$$\text{discharge} = \frac{c_1 \log_{10}(V(a))^{c_2}}{c_3^{c_2} + \log_{10}(V(a))^{c_2}} \quad (14)$$

provides a good description of the total amount of nasal discharge as function of virus load for human influenza A infections [58]. Here, the coefficients c_i describe the shape of the sigmoid curve. While the hosts in the present study are ducks, not humans, we submit that representing the total amount of discharge by a sigmoid curve makes inherent biological sense for any host. Multiplying virus load by the amount of discharge and integrating over the duration of infection gives

$$s_2 = \int_0^D V(a) \frac{c_1 \log_{10}(V(a))^{c_2}}{c_3^{c_2} + \log_{10}(V(a))^{c_2}} da. \quad (15)$$

For our numerical analysis below, we set $c_1 = 5$, $c_2 = 5$, $c_3 = 2.5$, which are values close to those previously determined by fit of this sigmoid curve to shedding data for humans [58]. The exact values for those coefficients matter little for the results we present in this study. Using the equation for s_2 instead of the equation for s_1 in equation (13) is an alternative for linking within-host dynamics to between-host fitness. Another plausible scenario is one where the rate of transmission is proportional to the logarithm of the virus load, giving

$$s_3 = \int_0^D \log(V(a)) da. \quad (16)$$

We can use this expression in equation (13) instead of s_1. Such a logarithmic dependence of transmission on virus load makes especially good sense given that $b_1(a)$ and therefore R_d are a measure for the number of new infections produced, which not only includes the shedding and transmission process, but also includes the probability that a subsequent infection in a new host is started. A logarithmic dependence between pathogen dose and the probability of infection occurring appears to be common [53,59–63]. Since it is not known which assumption for the link from within-host virus load to between-host transmission is most applicable to the host-pathogen system we study here, we will investigate all three possible functions s_j ($j = 1,2,3$) and their impact on host population level fitness as measured by R_0.

The environmental transmission component of fitness, R_e, can be linked to the within-host model in the same way as just described for the direct component, R_d. Specifically, we can write

$$R_e = \frac{b_2 S(0)}{c_b} \int_0^D w(a) da. \quad (17)$$

The rate of viral shedding into the environment, $w(a)$, again depends on the within-host dynamics. If we assume that $w(a)$ depends on the within-host virus load in the same way as the direct transmission rate $b_1(a)$, we obtain

$$R_e = \frac{b_2 S(0)}{c_b} h_2 s_j, \quad (18)$$

where the terms s_j represent the different link functions described in equations (12), (15) and (16), and h_2 is another constant of proportionality. Table 3 summarizes the important quantities we introduced in this section.

Model implementation

All statistical analyses and simulations were done in the R programming environment [64]. The scripts are available from the corresponding author's webpage (http://ahandel.myweb.uga.edu/resources.htm).

Results

Both the within- and between-host models contain a term for virus decay, namely c_w and c_b. It is obvious that to maximize fitness, the virus should minimize both c_w and c_b, i.e. it should be able to persist well both outside the host (in the air or on fomites for humans, in water for avian species) and inside the host. However, as we show below, there seem to be trade-offs between the ability to persist at low versus high temperatures. While higher temperatures lead to faster decay for all strains, some strains are better at persisting in the environment at low temperatures (low c_b), but this comes at the cost of rapid decay inside a host at higher temperatures (high c_w). In contrast, other strains seem to persist less well at low temperatures, but as temperature increases, their decay rate increases less rapidly, making them more stable at higher temperatures. Given this potential trade-off between c_w and c_b, we analyze how within- and between-host levels interact to determine overall virus fitness on the host population level as measured by $R_0 = R_d + R_e$. Within-host decay, c_w, affects within-host viral dynamics and thereby, through the link-functions s_j, both the direct and environmental fitness components R_d and R_e (equations 13 and 18). The between-host decay term, c_b, only affects the environmental fitness component, R_e. Therefore, we expect that depending on transmission route and link functions, the impact of good low- versus high-temperature persistence on fitness can change. We will show how this plays out in the following.

Temperature dependence of viral decay

In a recent study [33] we found that for a panel of different avian influenza A strains, the decay rate of infectious virus varies as a function of temperature. We can quantify the virus decay rate, c, as a function of temperature, T. The data suggest that a simple exponential function of the form $c(T) = \alpha e^{\gamma T}$ fits each strain well. Figure 3 shows the data and best-fit exponential curves, with the estimated values for α and γ provided in table 4. The simple equation $c(T) = \alpha e^{\gamma T}$ allows us to compute decay rates at a within-host temperature of around $40^{\circ}\mathrm{C}$ corresponding to the body temperature of a duck [15,65] and at a between-host environmental temperature assumed to be cold lake water at around $5^{\circ}\mathrm{C}$. Those quantities correspond to c_w and c_b in our within-host and between-host models. Table 4 lists their values for the different strains.

Figure 3 and table 4 suggest that while some strains have a relatively low (e.g. H3N2) or high (e.g. H5N2) decay rate irrespective of temperature, others appear to specialize. Some strains (e.g. H6N4, H11N6) decay relatively slowly at low temperatures but persist poorly at high temperatures, while others (e.g. H8N4, H7N6) do relatively better at high versus low temperature. Thus, some strains are able to persist for a long time at low temperatures, but as temperature increases, their rate of decay also rapidly increases. In contrast, other strains are not able to persist for quite as long at low temperatures, but increases in temperature leads to a slower rise in atrophy. As we illustrate in figure 4A, this can lead to a cross-over in decay rates as function of temperature. In figure 4B, we regress the strain-specific values for

Table 3. Summary of quantities linking the within-host and between-host scales.

symbol	meaning
h_1	constant of proportionality connecting virus load and direct transmission rate
h_2	constant of proportionality connecting virus load and environmental transmission rate
D	duration of infectiousness, obtained from the within-host model (equation 10)
s_1	link-function to connect virus load with transmission, assuming linear relation (equation 12)
s_2	link-function to connect virus load with transmission, assuming linear relation modified by total shedding (equation 15)
s_3	link-function to connect virus load with transmission, assuming logarithmic relation (equation 16)

doi:10.1371/journal.pcbi.1002989.t003

the intercept of the decay rate curve, α, (quantifying virus persistence at low temperature, specifically at $0^{\circ}C$) against the value for the temperature-dependence of the decay rate, γ, (quantifying virus persistence at high temperature). In figure 4C, we provide the same information, but for the rank of those parameters. These plots demonstrate a negative correlation between persistence at low and high temperatures. Since the center panel indicates a linear relation for the logarithm of α and γ, we fitted a regression line $\log(\gamma)=\eta+\kappa\log(\alpha)$ to the data. We find for the regression fit $\eta=-3.28$, $\kappa=-0.26$ ($R^2=0.70$, $p=0.00068$). Similarly, computing a correlation coefficient for the rank-transformed data, we find a negative correlation of -0.72 ($p=0.011$).

The analysis of this dataset can be taken as suggestion for the presence of a trade-off between stability at low and high temperatures – at least for the panel of strains we investigated here. Since this is a small sample of strains, we do not want to over-emphasize the finding. However it seemed real and interesting enough to ask the questio: "How would such a potential trade-off lead to interactions on the within-host and between-host levels and affect overall virus fitness?". We address this question in the remainder of the paper.

As a potentially interesting side question – not further considered in the remainder of this paper – we wondered whether there are systematic differences between strains belonging to different groups. Based on amino acid differences, strains with different HA types can be clustered into two groups, as indicated in Table 4 (see e.g. [66–68]). We were curious to see if systematic differences in the decay behavior between the two groups could be observed. However, statistical tests applied to both the absolute and rank-transformed values of α and γ did not identify significant differences between groups, suggesting that – based on the available data – differences in HA sequences between the two groups do not express themselves phenotypically as differences in temperature-dependent decay characteristics.

Fitting the within-host model

To simulate a within-host infection, we need to specify parameter values for the within-host model. While parameter estimates are available for influenza infections in humans and mice [41,42], they have not been previously estimated for ducks. We therefore fitted the model to recent data from influenza infections with H3N8 in mallards (*Anas platyrhynchos*) [69]. This virus strain was not used in the decay experiments shown in table 4, therefore, we do not have a direct estimate for the within-host clearance rate, c_w. The straightforward approach would be to obtain c_w together with the other parameters by fitting to the data, but this approach is problematic. As has been shown previously, it is impossible to use the within-host model (equations 1–3) to accurately estimate both c_w and death rate of infected cells, δ, from virus titer data alone [42,70]. Because of this, we instead set $c_w=2.78$ per day, which is the mean value of c_w for the 12 strains reported in table 4. We also tried to fit c_w, and as expected, the fit did not improve and c_w could not be properly estimated. To perform the fit, we assume that the infection was started by a 1 $\mathrm{EID}_{50}/\mathrm{mL}$ (EID_{50} is the viral dose that results in a 50% chance of infecting an embryonated egg, assumed to correspond to 1 infectious virion) and that the initial number of uninfected target cells is 2.5×10^7 [71] (while this estimate is for chickens rather than ducks, the exact value is not qualitatively important: changes in the target cell numbers only re-scale the model parameter p and otherwise produce the same dynamics). In figure 5, we show the best fit to the data, with parameter values presented in Table 1. We want to point out that while these parameter estimates are useful and accurate enough for the purpose of our study, they come with caveats. Most importantly, estimates are based on the validity of the model used. A model that does not include an immune response is likely an over-simplification, albeit a necessary one since adding additional immune response components and trying to fit such a model to virus load data only would lead to over-fitting. See e.g. [41,42] and references therein for further discussions of this and related points concerning fitting influenza data to models.

Determining between-host fitness

For each strain listed in table 4, we can use c_w and the parameters determined in the previous section and simulate the within-host infection dynamics. This allows us to numerically determine the duration of infection, D, and the total virus load, which in turn specifies the different link functions, s_j. We also have estimates for c_b for each strain. To determine fitness as measured by $R_0=R_d+R_e$, we also need to know the population size $S(0)$, and several constants of proportionality, namely h_1 and h_2 describing the linkage between within-host virus load and shedding and infection rates, and the environmental transmission rate, b_2. Those quantities are not well known and will likely differ for different environments. Therefore, absolute values of R_d and R_e are hard to estimate. However, for any strain n we can consider its fitness relative to some reference strain, $F^n=R_0^n/R_0^r$. If we make the assumption that for a given scenario, $S(0)$, h_1, h_2 and b_2 do not differ between strains; and consider the two extreme cases of either only direct ($h_2=0$) or only environmental ($h_1=0$) transmission, relative fitness for strain n and link-function j ($j=1,2,3$), relative to some reference strain, r, is given by

$$F^n_{\mathrm{direct,\ j}}=\frac{s_j^n}{s_j^r} \tag{19}$$

for direct transmission and

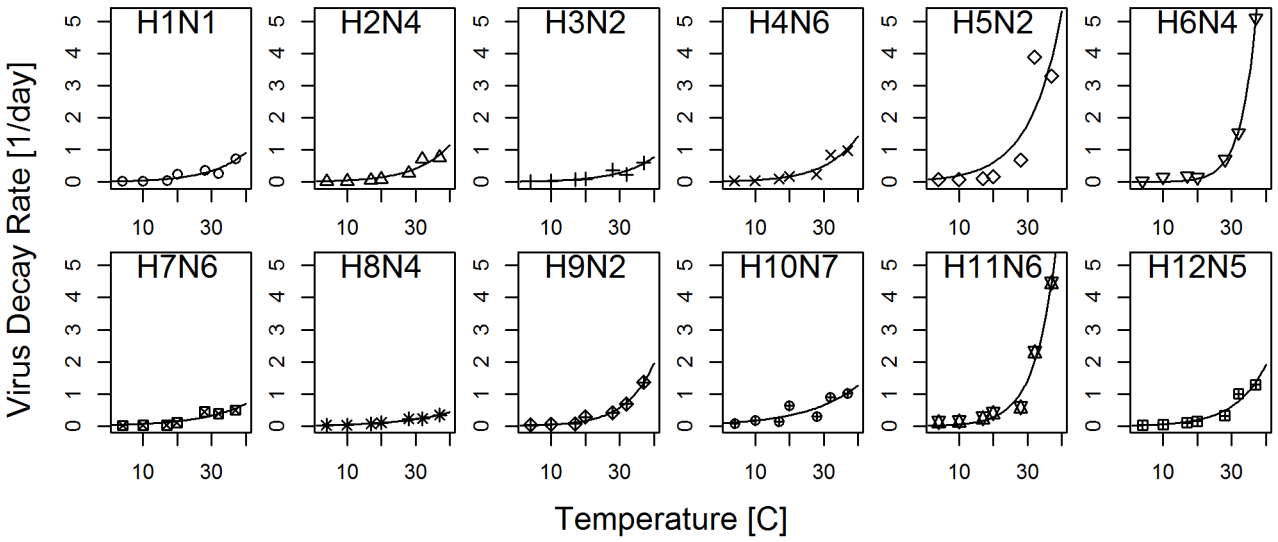

Figure 3. Decay rate for 12 different influenza strains as function of temperature. Symbols show data, lines show best fit of an exponential function. Virus decay for all strains was measured at the indicated temperature, a pH of 7.2, and salinity of 0. Decay for each strain was measured once for these specific conditions. See [33] for more experimental details.
doi:10.1371/journal.pcbi.1002989.g003

$$F^n_{\text{environmental, j}} = \frac{s_j^n c_b^r}{s_j^r c_b^n} \tag{20}$$

for indirect, environmental transmission. As expected, if we consider only direct transmission (equation 19), the ability of the virus to persist at low temperatures (low c_b) does not impact its fitness and therefore the strain that optimizes persistence at high temperatures (low c_w) and therefore optimizes within-host dynamics (large s_j) performs best. In the presence of environmental transmission (equation 20), fitness is influenced by persistence both inside the host (low c_w, leading to high s_j) and in the environment (low c_b).

The two cases, environmental only and direct only transmission represent extremes in terms of potential trade-offs. For direct transmission alone, there is no trade-off; optimizing within-host fitness is always the best strategy. The environmental transmission only scenario represents the case where the importance of the environmental stage is as large as it can possibly be. Mixture of the two transmission routes leads to values with intermediate importance of environmental persistence. While it is certainly possible to consider the general case with both direct and environmental transmission and compute absolute and relative fitness values, this would require making rather arbitrary assumptions about values for some of the unknown parameters of proportionality. Since considering such a general mixed transmission scenario would not add much beyond the results for the two simpler extreme cases, we focus on these two extreme cases in the following.

In figure 6, we show the relative fitness of the 12 different strains, for exclusively direct or environmental transmission scenarios. We plot relative fitness for the three different link-functions between within-host virus load and transmission/shedding described above (s_1, s_2 and s_3 given by equations (12), (15) and (16)). Strains are sorted according to within-host performance (i.e. with increasing values of c_w). We arbitrarily chose H1N1 as the reference strain, which therefore always has a fitness of 1. As expected, for direct transmission (figure 6A), better within host persistence at high temperatures leads overall to higher fitness. Results differ little between the link function based on the simple linear assumption, s_1, and the additional inclusion of total discharge, s_2. However, assuming that the amount of shedding is proportional to the logarithm of virus load, s_3, reduces the relative importance of within-host dynamics. Put another way, since s_3 "counts" $\log(V)$ instead of V, the fitness impacts of differences in within-host virus load between strains are diminished and, consequently, the relative fitness advantage of strains with high within-host persistence is reduced. This therefore increases the relative fitness of the

Table 4. Best fit values for the different influenza strains.

strain, (group)	α, (rank)	γ, (rank)	c_b, (rank)	c_w, (rank)
H1N1, (1)	0.019, (5)	0.097, (4)	0.031, (5)	0.914, (4)
H2N4, (1)	0.02, (7)	0.101, (6)	0.033, (6)	1.147, (5)
H3N2, (2)	0.015, (4)	0.098, (5)	0.025, (3)	0.772, (3)
H4N6, (2)	0.021, (8)	0.105, (7)	0.036, (8)	1.427, (7)
H5N2, (1)	0.07, (11)	0.108, (8)	0.121, (11)	5.316, (10)
H6N4, (1)	0.001, (1)	0.23, (12)	0.003, (1)	10.145, (12)
H7N6, (2)	0.034, (10)	0.076, (3)	0.049, (10)	0.697, (2)
H8N4, (1)	0.026, (9)	0.071, (2)	0.037, (9)	0.438, (1)
H9N2, (1)	0.014, (3)	0.123, (10)	0.027, (4)	1.948, (9)
H10N7, (2)	0.09, (12)	0.066, (1)	0.125, (12)	1.263, (6)
H11N6, (1)	0.011, (2)	0.163, (11)	0.025, (2)	7.334, (11)
H12N5, (1)	0.02, (6)	0.114, (9)	0.035, (7)	1.919, (8)

Best fit values for the different strains fitted to the function $c(T) = \alpha e^{\gamma T}$. Parameter γ is in units of 1/degree Celsius, α is in units of 1/day. Also shown are decay rates (units of 1/day) for each strain at 5 (c_b) and 40 (c_w) degrees Celsius. Numbers in parentheses following each strain indicate the genotype group (see main text). Numbers in parentheses following the other values indicate the rank of this value for each strain (with rank 1 given to the strain with the lowest value, corresponding to better persistence.)
doi:10.1371/journal.pcbi.1002989.t004

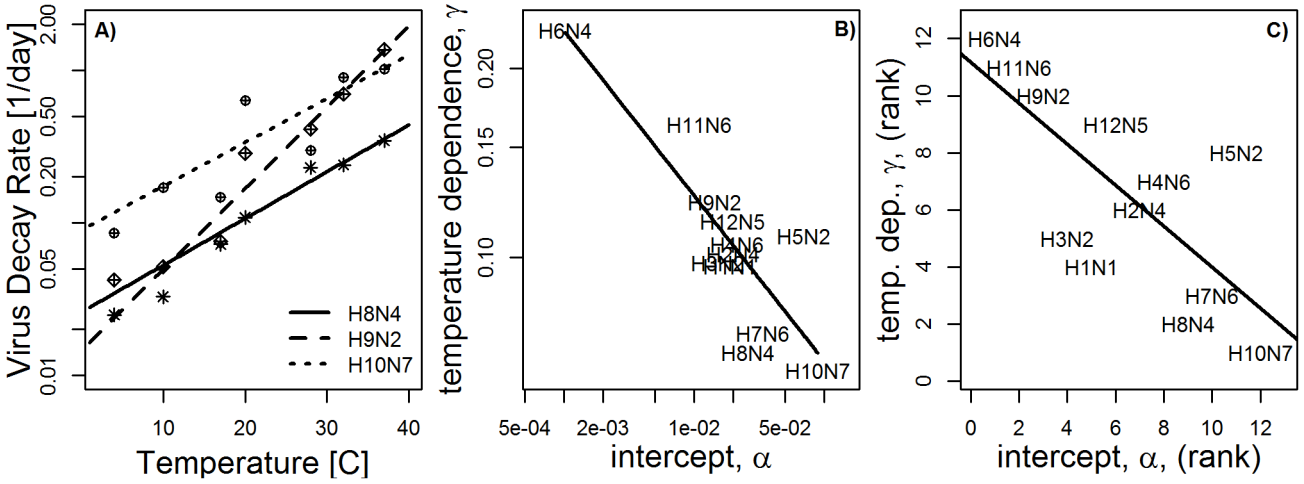

Figure 4. Temperature trade-off between strains. A) Decay rates for H8N4, H9N2 and H10N7, plotted on a log scale to illustrate the cross-over of decay rates. B) absolute values of α and γ for all strains, (note the log scale). C) Ranks of these parameters. Also plotted in each figure are regression lines.
doi:10.1371/journal.pcbi.1002989.g004

strains with high c_w. In fact, for the three strains with the lowest within-host fitness (H5N2, H11N6 and H6N4), the somewhat reduced within-host fitness due to higher c_w leads to lower virus load but a longer duration of infection, and because virus load factors into shedding only in a logarithmic fashion, a longer duration of infection leads to a slightly increased fitness despite higher c_w. See also the next section for another appearance of this phenomenon. Note that it is unclear how biologically reasonable sustained within-host virus load (i.e. a long duration of infection) is. In most immunocompentent hosts, the immune response usually clears influenza relatively rapidly [72–77]. In the supplementary materials, we investigate an extended within-host model which includes an antibody-mediated immune response.

Not surprisingly, for the environmental transmission scenario (figure 6B), the trend of higher overall fitness for the strains with better within-host persistence is less pronounced. For instance, the H7N6 strain is the second fittest strain for the direct transmission scenario, but is surpassed in fitness for the environmental transmission scenario by several other strains with better low-temperature persistence. Again, results for the different link functions are rather similar. The one outlier is H6N4, which has the best low-temperature and worst high-temperature persistence. For this strain and link function s_3, the reduction in relative importance of the high-temperature within-host dynamics compared to the low-temperature between-host persistence strongly increases this strain's relative fitness (see top left corner of figure 6B).

General trade-off for viral decay

So far, we analyzed decay data for specific influenza strains and documented differences in their ability to persist well at low and high temperatures. We can go one step further and study the hypothetical fitness of strains that we did not measure. To do so, we can vary α (i.e. clearance rate at $0\,^{\circ}\mathrm{C}$) over a wide range of values, and for each value we can compute a corresponding γ according to the regression equation $\log(\gamma)=\eta+\kappa\log(\alpha)$ estimated above. We then use the values of α and γ to compute virus decay rate, $c(T)=\alpha e^{\gamma T}$ (specifically, c_b and c_w at 5 and 40 degrees Celsius). These values for both the actual virus isolates and the theoretical model are shown in figure 7. The figure shows that not surprisingly, as α (clearance rate at $0\,^{\circ}\mathrm{C}$) increases, clearance rate c_b at a close-by low temperature ($5\,^{\circ}\mathrm{C}$) also increases. In contrast, as α increases (worse low-temperature persistence), the trade-off leads to a decrease of the within-host clearance rate, c_w, (better high-temperature persistence) – at least initially: At high enough α, within-host clearance rate starts to increase again. Mathematically, this is due to the fact that at large α and small γ, the linear term in

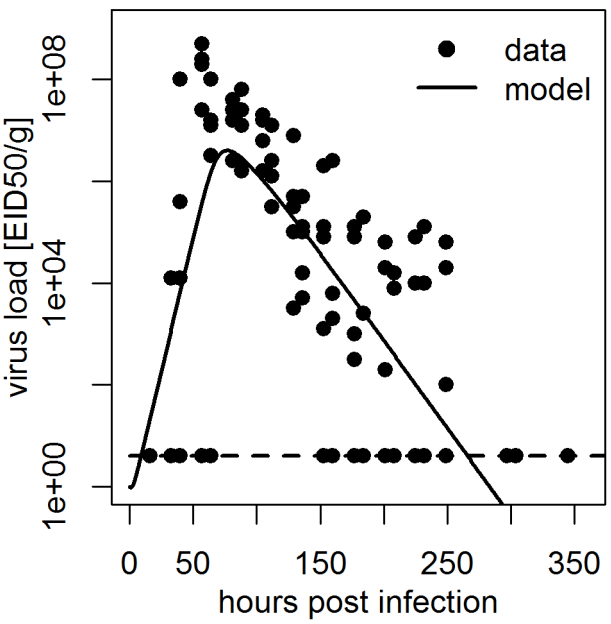

Figure 5. Best fit of within-host model to fecal virus load from influenza infections of mallards (Anas Platyrhynchos). The limit of detection for the virus load was 4 EID_{50} (EID_{50} = 50% Egg Infectious Doses) and is indicated by the dashed horizontal line. See [69] for more details on the experiments and data. Fitting was done using a least squares approach for the logarithm of the virus load, corresponding to the assumption of log-normally distributed errors [89]. For data at the limit of detection (i.e. left-censored data), differences between model and data were accounted for if the model was above the data point, but not if the model took on any value below the limit of detection [75].
doi:10.1371/journal.pcbi.1002989.g005

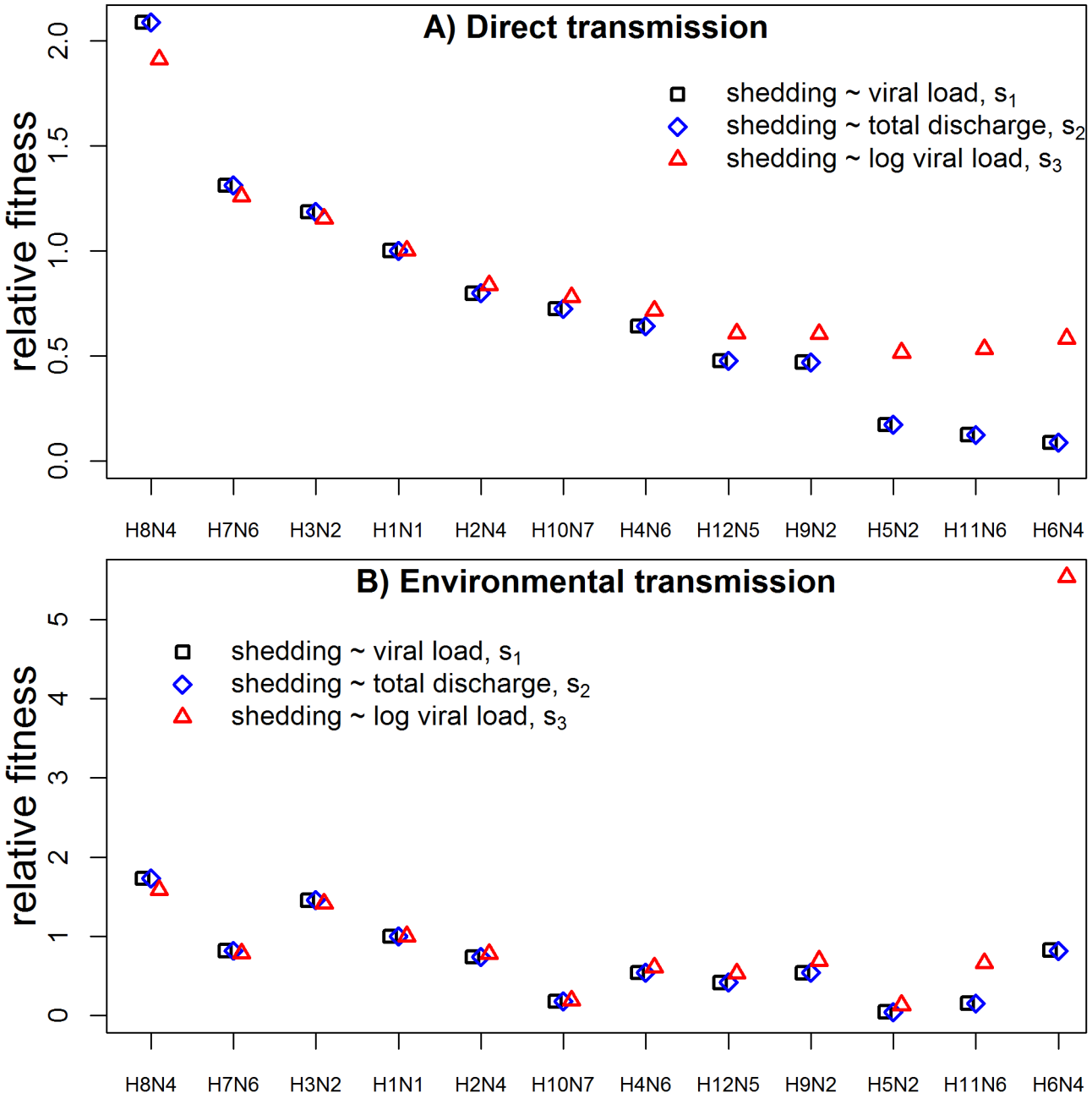

Figure 6. Relative Fitness for the 12 influenza strains. A) direct transmission (equation 19) and B) environmental transmission (equation 20) scenarios. We plot fitness for the three different link functions, s_j, between within-host virus load and transmission/shedding described in the model section, i.e. s_1, s_2 and s_3 given by equations (12), (15) and (16). Strains are sorted according to within-host fitness, with H8N4 having the best within-host fitness (i.e. lowest value of c_w, see Table 4). We arbitrarily chose H1N1 as the reference strain, which therefore has a relative fitness of 1.
doi:10.1371/journal.pcbi.1002989.g006

the decay equation $c(T)=\alpha e^{\gamma T}$ dominates. Biologically, this indicates a strain with poor persistence largely independent of the temperature (i.e. both large c_b and c_w). In our dataset, H5N2 seems to fit this description.

To determine between-host fitness for a generic strain with given α and γ values, we use c_w for every value of α and simulate the within-host infection model, compute duration of infection and total virus load, determine the link functions s_j, and finally compute fitness as quantified by R_e and R_d. We normalize fitness to 1 to cancel out the different constants of proportionality, as done previously. Figure 8 shows normalized fitness for direct and environmental transmission for the different link functions s_j. For s_1 and s_2, results are virtually indistinguishable. For both s_1 and s_2, an intermediate level of α leads to optimal fitness. For direct transmission, with fitness measured by R_d, the maximum fitness directly corresponds to the value of α at which c_w is lowest (see figure 7B). For environmental transmission, the maximum fitness is shifted towards lower α (i.e. lower c_b) values, meaning better persistence at low temperatures becomes important.

For the scenario where shedding and infection rate are proportional to the logarithm of virus load (s_3) one finds that for environmental transmission, within-host dynamics plays a minor role and persistence

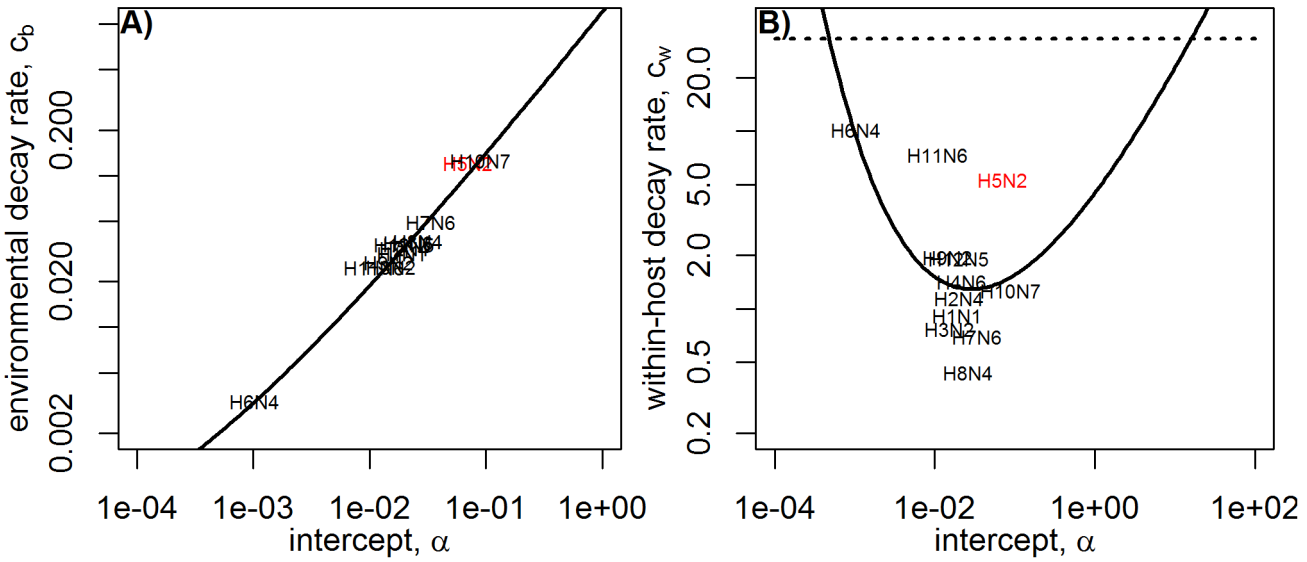

Figure 7. Virus decay rate at different temperatures. A) environmental, between-host temperature, c_b, and B) within-host temperature, c_w, as a function of α (decay rate at 0 degrees Celsius). Solid lines are theoretical values obtained by choosing a value of α and computing the corresponding value for γ from the regression equation $\log(\gamma)=\eta+\kappa\log(\alpha)$, where the values for $\eta=-3.28$ and $\kappa=-.026$ are the best-fit values obtained previously by fitting the decay data for the different strains. The dashed horizontal line indicates the level of c_w above which within-host fitness is so small that no infection takes place. H5N2 is highlighted as a strain with poor persistence at both low and high temperatures – see text.
doi:10.1371/journal.pcbi.1002989.g007

at low temperatures (low α) is the dominating component for fitness. Direct transmission for the s_3 link function produces the most interesting pattern. While this scenario shows a local maximum at medium α like those seen for s_1 and s_2 link functions, fitness is highest for either low or high α, close to the edge at which within-host infection becomes impossible. This is because at those values, virus load is low but the duration of infection is rather long. As explained in the previous section, the long duration of infection can more than make up for the reduced virus levels, leading to an overall increase in s_3 and therefore explaining the high fitness at the edges. The pronounced fitness peaks resulting from long-lasting infections are not seen in a within-host model that includes an immune response (see supplementary materials), and are therefore likely not relevant for influenza in immunocompetent hosts. However, such a long-lasting infection might have relevance for immunocompromised hosts, and is likely important for other pathogens (see e.g. the "sexually transmitted infection regime" in [53]).

Discussion

Trade-offs between different traits or phenotypes acting at different scales are likely common and have been explored

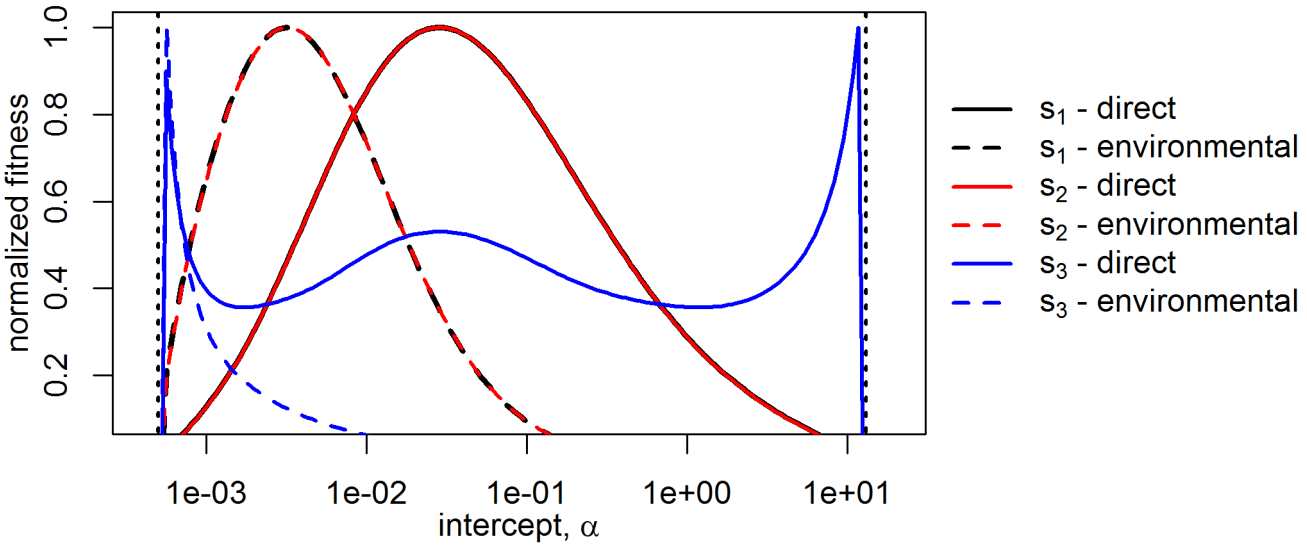

Figure 8. Normalized Fitness as measured by R_d and R_e for direct transmission and environmental transmission. The dashed vertical lines indicate the level of α above which c_w becomes so large that no infection takes place (c.f. horizontal line in figure 7). Note that results for s_1 and s_2 are virtually indistinguishable and therefore the curves are on top of each other.
doi:10.1371/journal.pcbi.1002989.g008

previously (see e.g. [9,10,40,53,58,78–88] for some recent work). In this study, we focused on trade-offs in temperature-dependent virus decay and analyzed how the interaction of within- and between-host scales determines overall fitness. Taking a panel of influenza A strains, we found evidence that a trade-off exists between the ability to persist at low temperatures versus high temperatures. Of course, the negative correlation found in the data should by no means be taken as proof of the existence of such a trade-off. Further, more detailed studies are needed to investigate this potential trade-off more carefully. If the finding holds up, it would also be very interesting to elucidate the mechanism responsible for this trade-off. As it currently stands, we consider the observed pattern as an interesting suggestion that made it worthwhile to investigate how – given such a trade-off – the within-host and between-host scales interact to impact overall fitness. By linking the within-host dynamics to the population level, we were able to estimate population level-fitness as measured by the reproductive number for both the cases where transmission is through direct contact between birds and where transmission occurs through an environmental stage (i.e. virus persistence in water). We found that if direct transmission is dominant, viruses that persist well at high temperatures and therefore perform well within a host also had the best between-host fitness. This trend was most pronounced if transmission or shedding was directly proportional to the total within-host virus load. For the environmental transmission scenario, the balance was somewhat shifted toward viruses with good environmental, low-temperature, persistence. This was especially true if shedding and infection rate were assumed to be proportional to the logarithm of the virus load.

In the supplementary materials, we also explored the impacts of taking into account an immune response. We found a somewhat diminished importance of differences in the between-host decay rate between strains. This, in turn, leads to greater emphasis on the fitness contribution of environmental persistence. Along similar lines, a brief analysis of a model including virulence suggests that if high within-host fitness leads to host death and thereby interruption of transmission, the balance would be further tipped toward strains that have good environmental persistence.

Both more detailed within-host models including further aspects of the immune response and more detailed virulence models are worthwhile avenues for further studies. So are models with more detailed links of the within-host and between-host scales. However, to go beyond qualitative results, the right kind of data would need to be available to allow proper specification and parameterization of such more complex models.

In addition, it will be worthwhile to follow up with studies that look at virus fitness beyond the reproductive number. Specifically, given the epidemic behavior of influenza, a model that would explicitly simulate multiple rounds of seasonal between-host outbreaks (along the lines of [16]) and track persistence and extinction of strains with different temperature-dependent persistence strategies might be insightful. Similarly, a more detailed model of environmental persistence, e.g. through inclusion of seasonal variation and other dynamical features, and its effect on fitness as measured by the reproductive number or some other suitable quantity might be of interest.

Another fruitful topic for future studies is to investigate additional potential trade-offs. It is known that temperature has an effect on other phenotypes, such as virus binding efficiency or the performance of polymerase. This could be included in a model by making other model parameters temperature-dependent. Provided the right kind of data were available, one could then study how temperature impacts these additional parameters and thereby overall fitness.

In summary, our results show that differences in fitness can at times be substantial and strongly depend on transmission route and how within-host and between-host models are linked. Based on our findings, we predict that if shedding and infection rates are proportional to virus load, virulence is negligible, and within-host virus clearance is primarily determined by temperature-dependent virus decay, there is strong evolutionary pressure for influenza viruses to increase persistence at high temperatures. Conversely, if virus shedding and direct transmission rates scale with the logarithm of virus load, if virulence plays an important role, or if within-host virus clearance is essentially via the immune response or other non-temperature dependent mechanisms, influenza viruses with good environmental persistence at low temperatures should be favored.

Supporting Information

Figure S1 Flow diagram for the within-host model with a B-cell/antibody immune response. U, X, V and B are the variables describing uninfected cells, infected cells, virus and B-cells/antibodies. Uninfected cells become infected at rate k, infected cells produce virus at rate p and die at rate δ. Virus decays at rate c_W. B-cells/antibodies expand exponentially through clonal expansion at rate r and remove virus at rate q. Solid lines indicate physical flows, dashed lines indicate interactions.
(TIFF)

Figure S2 Relative fitness for different strengths of the immune response. Left column shows direct transmission scenarios, right column shows environmental transmission scenarios. The rows show from top to bottom the different forms of linking within-host virus load to between-host transmission, i.e. s_1, s_2, s_3. Note that for clarity of representation, we use a linear scale for the direct and a log scale for the environmental transmission scenario.
(TIFF)

Figure S3 Fitness as measured by R_d and R_e (normalized to 1) for direct transmission and environmental transmission, with immune response at $q=10^{-1}$. The dashed vertical lines indicate the levels of α where c_w becomes so large that no infection takes place. Note that results for s_1 and s_2 are virtually indistinguishable and therefore the curves are on top of each other.
(TIFF)

Figure S4 Relative fitness for the A) direct and B) environmental transmission scenario for different shedding definitions in the presence of virulence. Fitness for H6N4 in the environmental transmission scenario with link-function s_3 is 50 and not shown on the plot.
(TIFF)

Text S1 Additional Results for a within-model including an immune response and a scenario including virulence.
(PDF)

Acknowledgments

We thank the reviewers for comments that helped to greatly improve the article.

Author Contributions

Conceived and designed the experiments: AH PR. Performed the experiments: AH. Analyzed the data: AH. Contributed reagents/materials/analysis tools: JB DS PR. Wrote the paper: AH PR.

References

1. Cox NJ, Subbarao K (2000) Global epidemiology of influenza: past and present. Annu Rev Med 51: 407–421.
2. Nicholson KG, Wood JM, Zambon M (2003) Influenza. The Lancet 362: 1733–1745.
3. Taubenberger JK, Morens DM (2008) The pathology of influenza virus infections. Annu Rev Pathol 3: 499–522.
4. Thompson WW, Shay DK, Weintraub E, Brammer L, Cox N, et al. (2003) Mortality associated with influenza and respiratory syncytial virus in the United States. JAMA 289: 179–186.
5. Webster RG, Bean WJ, Gorman OT, Chambers TM, Kawaoka Y (1992) Evolution and ecology of influenza A viruses. Microbiol Rev 56: 152–179.
6. Horimoto T, Kawaoka Y (2005) Influenza: lessons from past pandemics, warnings from current incidents. Nat Rev Microbiol 3: 591–600.
7. Lewis DB (2006) Avian flu to human influenza. Annu Rev Med 57: 139–154.
8. Palese P (2004) Influenza: old and new threats. Nature Medicine 10: S82–S87.
9. Mideo N, Alizon S, Day T (2008) Linking within- and between-host dynamics in the evolutionary epidemiology of infectious diseases. Trends Ecol Evol 23: 511–517.
10. Alizon S, Luciani F, Regoes RR (2011) Epidemiological and clinical consequences of within-host evolution. Trends Microbiol 19: 24–32.
11. Reperant LA, Kuiken T, Grenfell BT, Osterhaus ADME, Dobson AP (2012) Linking influenza virus tissue tropism to population-level reproductive fitness. PLoS One 7: e43115.
12. Belshe RB, Mendelman PM, Treanor J, King J, Gruber WC, et al. (1998) The efficacy of live attenuated, cold-adapted, trivalent, intranasal influenza virus vaccine in children. N Engl J Med 338: 1405–1412.
13. Cox RJ, Brokstad KA, Ogra P (2004) Influenza virus: immunity and vaccination strategies. comparison of the immune response to inactivated and live, attenuated influenza vaccines. Scand J Immunol 59: 1–15.
14. Lowen AC, Mubareka S, Steel J, Palese P (2007) Influenza virus transmission is dependent on relative humidity and temperature. PLoS Pathog 3: 1470–1476.
15. Scull MA, Gillim-Ross L, Santos C, Roberts KL, Bordonali E, et al. (2009) Avian influenza virus glycoproteins restrict virus replication and spread through human airway epithelium at temperatures of the proximal airways. PLoS Pathog 5: e1000424.
16. Breban R, Drake JM, Stallknecht DE, Rohani P (2009) The role of environmental transmission in recurrent avian influenza epidemics. PLoS Comput Biol 5: e1000346.
17. Rohani P, Breban R, Stallknecht DE, Drake JM (2009) Environmental transmission of low pathogenicity avian influenza viruses and its implications for pathogen invasion. Proc Natl Acad Sci U S A 106: 10365–10369.
18. Breban R, Drake JM, Rohani P (2010) A general multi-strain model with environmental transmission: invasion conditions for the disease-free and endemic states. J Theor Biol 264: 729–736.
19. Roche B, Lebarbenchon C, Gauthier-Clerc M, Chang CM, Thomas F, et al. (2009) Water-borne transmission drives avian influenza dynamics in wild birds: the case of the 2005–2006 epidemics in the camargue area. Infect Genet Evol 9: 800–805.
20. Farnsworth ML, Miller RS, Pedersen K, Lutman MW, Swafford SR, et al. (2012) Environmental and demographic determinants of avian influenza viruses in waterfowl across the contiguous united states. PLoS One 7: e32729.
21. Lebarbenchon C, Yang M, Keeler SP, Ramakrishnan MA, Brown JD, et al. (2011) Viral replication, persistence in water and genetic characterization of two influenza a viruses isolated from surface lake water. PLoS One 6: e26566.
22. Hnaux V, Samuel MD, Bunck CM (2010) Model-based evaluation of highly and low pathogenic avian influenza dynamics in wild birds. PLoS One 5: e10997.
23. Hnaux V, Samuel MD (2011) Avian influenza shedding patterns in waterfowl: implications for surveillance, environmental transmission, and disease spread. J Wildl Dis 47: 566–578.
24. Stallknecht DE, Goekjian VH, Wilcox BR, Poulson RL, Brown JD (2010) Avian influenza virus in aquatic habitats: what do we need to learn? Avian Dis 54: 461–465.
25. Atkinson MP, Wein LM (2008) Quantifying the routes of transmission for pandemic influenza. Bull Math Biol 70: 820–867.
26. Nicas M, Jones RM (2009) Relative contributions of four exposure pathways to influenza infection risk. Risk Anal 29: 1292–1303.
27. Wagner BG, Coburn BJ, Blower S (2009) Calculating the potential for within-ight transmission of influenza a (h1n1). BMC Med 7: 81.
28. Weber TP, Stilianakis NI (2008) Inactivation of influenza a viruses in the environment and modes of transmission: a critical review. J Infect 57: 361–373.
29. Tang JW (2009) The effect of environmental parameters on the survival of airborne infectious agents. J R Soc Interface 6 Suppl 6: S737–S746.
30. Stallknecht DE, Kearney MT, Shane SM, Zwank PJ (1990) Effects of ph, temperature, and salinity on persistence of avian influenza viruses in water. Avian Dis 34: 412–418.
31. Stallknecht DE, Shane SM, Kearney MT, Zwank PJ (1990) Persistence of avian influenza viruses in water. Avian Dis 34: 406–411.
32. Brown JD, Swayne DE, Cooper RJ, Burns RE, Stallknecht DE (2007) Persistence of h5 and h7 avian influenza viruses in water. Avian Dis 51: 285–289.
33. Brown JD, Goekjian G, Poulson R, Valeika S, Stallknecht DE (2009) Avian influenza virus in water: infectivity is dependent on ph, salinity and temperature. Vet Microbiol 136: 20–26.
34. Bonhoeffer S, Lenski RE, Ebert D (1996) The curse of the pharaoh: the evolution of virulence in pathogens with long living propagules. Proc Biol Sci 263: 715–721.
35. Gandon S (1998) The curse of the pharaoh hypothesis. Proc Biol Sci 265: 1545–1552.
36. Day T (2002) Virulence evolution via host exploitation and toxin production in spore-producing pathogens. Ecology Letters 5: 471–476.
37. Handel A, Bennett MR (2008) Surviving the bottleneck: transmission mutants and the evolution of microbial populations. Genetics 180: 2193–2200.
38. Caraco T, Wang IN (2008) Free-living pathogens: life-history constraints and strain competition. J Theor Biol 250: 569–579.
39. Walther BA, Ewald PW (2004) Pathogen survival in the external environment and the evolution of virulence. Biol Rev Camb Philos Soc 79: 849–869.
40. Paepe MD, Taddei F (2006) Viruses' life history: towards a mechanistic basis of a trade-off between survival and reproduction among phages. PLoS Biol 4: e193.
41. Smith AM, Perelson AS (2011) Influenza a virus infection kinetics: quantitative data and models. Wiley Interdiscip Rev Syst Biol Med 3: 429–445.
42. Beauchemin CAA, Handel A (2011) A review of mathematical models of influenza A infections within a host or cell culture: lessons learned and challenges ahead. BMC Public Health 11 Suppl 1: S7.
43. Bonhoeffer S, Herz AV, Boerlijst MC, Nee S, Nowak MA, et al. (1996) Explaining "linguistic features" of noncoding DNA. Science 271: 14–15.
44. Joh RI, Wang H, Weiss H, Weitz JS (2009) Dynamics of indirectly transmitted infectious diseases with immunological threshold. Bull Math Biol 71: 845–862.
45. Kamo M, Boots M (2004) The curse of the pharaoh in space: free-living infectious stages and the evolution of virulence in spatially explicit populations. J Theor Biol 231: 435–441.
46. Li S, Eisenberg JNS, Spicknall IH, Koopman JS (2009) Dynamics and control of infections transmitted from person to person through the environment. Am J Epidemiol 170: 257–265.
47. Anderson RM, May RM (1991) Infectious Diseases of Humans - Dynamics and Control. Oxford: Oxford Science Publications.
48. Keeling M, Rohani P (2007) Modeling Infectious Diseases in Humans and Animals. Princeton University Press.
49. Heffernan JM, Smith RJ, Wahl LM (2005) Perspectives on the basic reproductive ratio. J R Soc Interface 2: 281–293.
50. Alexander DJ (2000) A review of avian influenza in different bird species. Vet Microbiol 74: 3–13.
51. Swayne DE, editor (2008) Avian Influenza, 1st edition. Wiley-Blackwell.
52. Majumdar SK, Brenner FJ, Huffman JE, McLean RG, Panah AI, et al (2011) Pandemic Influenza Viruses: Science, Surveillance and Public Health. Pennsylvania Academy of Science.
53. Lange A, Ferguson NM (2009) Antigenic diversity, transmission mechanisms, and the evolution of pathogens. PLoS Comput Biol 5: e1000536.
54. Chen SC, Chio CP, Jou LJ, Liao CM (2009) Viral kinetics and exhaled droplet size affect indoor transmission dynamics of influenza infection. Indoor Air 19: 401–413.
55. Hall CB, Douglas R Jr, Geiman JM, Meagher MP (1979) Viral shedding patterns of children with influenza b infection. J Infect Dis 140: 610–613.
56. Spicknall IH, Koopman JS, Nicas M, Pujol JM, Li S, et al. (2010) Informing optimal environmental influenza interventions: how the host, agent, and environment alter dominant routes of transmission. PLoS Comput Biol 6: e1000969.
57. Halloran SK, Wexler AS, Ristenpart WD (2012) A comprehensive breath plume model for disease transmission via expiratory aerosols. PLoS One 7: e37088.
58. Handel A, Longini IM, Antia R (2007) Neuraminidase Inhibitor Resistance in Influenza: Assessing the Danger of Its Generation and Spread. PLoS Comput Biol 3: e240.
59. Haas CN (1983) Estimation of risk due to low doses of microorganisms: a comparison of alternative methodologies. Am J Epidemiol 118: 573–582.
60. Quinn TC, Wawer MJ, Sewankambo N, Serwadda D, Li C, et al. (2000) Viral load and heterosexual transmission of human immunodeficiency virus type 1. rakai project study group. N Engl J Med 342: 921–929.
61. Hollingsworth TD, Anderson RM, Fraser C (2008) Hiv-1 transmission, by stage of infection. J Infect Dis 198: 687–693.
62. Ben-Ami F, Regoes RR, Ebert D (2008) A quantitative test of the relationship between parasite dose and infection probability across different host-parasite combinations. Proc Biol Sci 275: 853–859.
63. Ssematimba A, Hagenaars TJ, de Jong MCM (2012) Modelling the wind-borne spread of highly pathogenic avian influenza virus between farms. PLoS One 7: e31114.
64. R Development Core Team (2011) R: A Language and Environment for Statistical Computing. R Foundation for Statistical Computing, Vienna, Austria. URL http://www.R-project.org/. ISBN 3-900051-07-0.
65. Marais M, Gugushe N, Maloney SK, Gray DA (2011) Body temperature responses of pekin ducks (anas platyrhynchos domesticus) exposed to different pathogens. Poult Sci 90: 1234–1238.

66. Throsby M, van den Brink E, Jongeneelen M, Poon LLM, Alard P, et al. (2008) Heterosubtypic neutralizing monoclonal antibodies cross-protective against h5n1 and h1n1 recovered from human igm+ memory b cells. PLoS One 3: e3942.
67. Russell RJ, Kerry PS, Stevens DJ, Steinhauer DA, Martin SR, et al. (2008) Structure of influenza hemagglutinin in complex with an inhibitor of membrane fusion. Proc Natl Acad Sci U S A 105: 17736–17741.
68. Corti D, Voss J, Gamblin SJ, Codoni G, Macagno A, et al. (2011) A neutralizing antibody selected from plasma cells that binds to group 1 and group 2 influenza a hemagglutinins. Science 333: 850–856.
69. Brown JD, Berghaus RD, Costa TP, Poulson R, Carter DL, et al. (2012) Intestinal excretion of a wild bird-origin h3n8 low pathogenic avian influenza virus in mallards (anas platyrhynchos). J Wildl Dis 48: 991–998.
70. Smith AM, Adler FR, Perelson AS (2010) An accurate two-phase approximate solution to an acute viral infection model. J Math Biol 60: 711–726.
71. Uni Z, Ganot S, Sklan D (1998) Posthatch development of mucosal function in the broiler small intestine. Poult Sci 77: 75–82.
72. Baccam P, Beauchemin C, Macken CA, Hayden FG, Perelson AS (2006) Kinetics of influenza A virus infection in humans. J Virol 80: 7590–7599.
73. Lee HY, Topham DJ, Park SY, Hollenbaugh J, Treanor J, et al. (2009) Simulation and prediction of the adaptive immune response to influenza a virus infection. J Virol 83: 7151–7165.
74. Saenz RA, Quinlivan M, Elton D, Macrae S, Blunden AS, et al. (2010) Dynamics of influenza virus infection and pathology. J Virol 84: 3974–3983.
75. Handel A, Longini IM, Antia R (2010) Towards a quantitative understanding of the within-host dynamics of influenza A infections. J R Soc Interface 7: 35–47.
76. Miao H, Hollenbaugh JA, Zand MS, Holden-Wiltse J, Mosmann TR, et al. (2010) Quantifying the early immune response and adaptive immune response kinetics in mice infected with influenza a virus. J Virol 84: 6687–6698.
77. Pawelek KA, Huynh GT, Quinlivan M, Cullinane A, Rong L, et al. (2012) Modeling within-host dynamics of influenza virus infection including immune responses. PLoS Comput Biol 8: e1002588.
78. Coombs D, Gilchrist MA, Ball CL (2007) Evaluating the importance of within- and between-host selection pressures on the evolution of chronic pathogens. Theor Popul Biol 72: 576–591.
79. Gilchrist MA, Coombs D (2006) Evolution of virulence: interdependence, constraints, and selection using nested models. Theor Popul Biol 69: 145–153.
80. Luciani F, Sisson SA, Jiang H, Francis AR, Tanaka MM (2009) The epidemiological fitness cost of drug resistance in mycobacterium tuberculosis. Proc Natl Acad Sci U S A 106: 14711–14715.
81. Day T, Alizon S, Mideo N (2011) Bridging scales in the evolution of infectious disease life histories: theory. Evolution 65: 3448–3461.
82. Mideo N, Savill NJ, Chadwick W, Schneider P, Read AF, et al. (2011) Causes of variation in malaria infection dynamics: insights from theory and data. Am Nat 178: E174–E188.
83. Read JM, Keeling MJ (2006) Disease evolution across a range of spatio-temporal scales. Theor Popul Biol 70: 201–213.
84. King AA, Shrestha S, Harvill ET, Bjrnstad ON (2009) Evolution of acute infections and the invasion-persistence trade-off. Am Nat 173: 446–455.
85. Klinkenberg D, Heesterbeek JAP (2007) A model for the dynamics of a protozoan parasite within and between successive host populations. Parasitology 134: 949–958.
86. Pepin KM, Volkov I, Banavar JR, Wilke CO, Grenfell BT (2010) Phenotypic differences in viral immune escape explained by linking within-host dynamics to host-population immunity. J Theor Biol 265: 501–510.
87. Steinmeyer SH, Wilke CO, Pepin KM (2010) Methods of modelling viral disease dynamics across the within- and between-host scales: The impact of virus dose on host population immunity. Philos Trans R Soc Lond B Biol Sci 365: 1931–1941.
88. Volkov I, Pepin KM, Lloyd-Smith JO, Banavar JR, Grenfell BT (2010) Synthesizing within-host and population-level selective pressures on viral populations: the impact of adaptive immunity on viral immune escape. J R Soc Interface 7: 1311–1318.
89. Bolker BM (2008) Ecological Models and Data in R. Princeton University Press.